

TABLE III. A summary of results for the reduced widths and from the considerations of isobaric spin.

Level	J	T	Reduced width	Single-particle limit	Energy calculated from S^{35} analog levels (MeV)	Resonance strength	T splitting	V_1 (MeV)
7.54	$\frac{7}{2}$	$\frac{3}{2}$	$\theta_p^2 = 0.2 \pm 0.1^a$	$\theta_p^2 = 0.33$	7.35	2.6 ± 0.4 eV	4.38 MeV	102
3.16	$\frac{7}{2}$	$\frac{1}{2}$						
7.84	$\frac{3}{2}$	$\frac{3}{2}$	$\theta_p^2 = 0.2 \pm 0.1^a$	$\theta_p^2 = 0.33$	7.89	3.4 ± 0.6 eV	3.67 MeV	86
4.17	$\frac{3}{2}$	$\frac{1}{2}$						

^a Recent calculations of the reduced widths using a computer code from J. P. Schiffer of Argonne National Laboratory have resulted in the value 0.20 ± 0.02 for the reduced width of the 7.84-MeV level. This result is based upon a nuclear radius of $1.4 (A^{1/3} + 1)$ F. Because of the uncertainty in the experimental value of the proton width of the 7.54-MeV level, we were unable to obtain a more accurate value of its reduced width.

in the neighborhood of the 1214- and 1512-keV resonances together with the large reduced widths of these resonances indicates that the single-particle excitations are not mixing to any appreciable extent with nearby $T = \frac{1}{2}$ states of the same spin and parity. Evidently at

this low excitation energy the $T = \frac{1}{2}$ states are still widely spaced relative to the strength of the isospin breaking interactions, although at higher excitation energies there is some evidence for isospin mixing. Further investigation of these effects is now in progress.

Energy Dependence of $(p, p' \gamma)$ Correlations in Ti^{48} †

H. J. HAUSMAN, R. M. HUMES,* AND R. G. SEYLER

The Ohio State University, Columbus, Ohio

(Received 27 July 1967)

Absolute double-differential cross sections have been measured at ten bombarding energies from 4–6 MeV for the reaction $\text{Ti}^{48}(p, p' \gamma)0.99$ MeV. The angular correlations were measured with the γ -ray detector moving in a plane perpendicular to the reaction plane. Comparisons are made between the measured cross sections and the predictions of the statistical compound-nucleus theory. At all bombarding energies, angular correlations were measured at two supplementary (c.m.) proton-detector angles in order to check the symmetries predicted by statistical theory. Attempts are made to ascribe deviations of the experimental correlations from statistical-model predictions to the presence of direct reactions. The angular dependence of the spin-flip cross section was measured at three bombarding energies: 5.16, 5.25, and 5.46 MeV. In addition, the energy dependence of the spin-flip cross section was measured at a laboratory proton-detector angle of 131° . For that geometry wherein the proton detector is in the backward quadrant, agreement between the measured correlations and statistical-model predictions is very good.

I. INTRODUCTION

IN recent years there has been considerable interest in the study of angular (triple) correlations between inelastically scattered nucleons and their associated de-excitation γ rays as a tool for studying reaction mechanisms. Many of these studies have been made at relatively high energies with consequent comparison to direct interaction (DI) theory. Sheldon¹ has shown, however, that in many of these cases, especially for atomic masses greater than 40, the results may be fitted reasonably well by statistical compound-nucleus (CN) correlation theory.

As a more sensitive test for the admixture of CN and

DI mechanisms, Sheldon^{1,2} has suggested the study of noncoplanar radiations. In a previous paper³ in which the angular dependence of the correlation function for Ti^{48} was studied at two energies, the authors noted an apparent symmetry breakdown which indicated that the normal-plane correlation function may provide a more sensitive measure of the CN-DI admixture than reaction-plane correlations. The present paper reports the extension of these normal-plane correlations to a series of ten bombarding energies corresponding to peaks and valleys in the excitation curve above and below the Coulomb barrier and the (p, n) threshold.

Model-independent symmetries associated with particle- γ -ray angular correlations can, in certain circumstances, aid in the analysis of reaction mechanisms.

† This work was supported in part by the National Science Foundation under Grant No. GP-2210.

* Present address: Pacific Northwest Laboratory, Richland, Washington.

¹ E. Sheldon, *Rev. Mod. Phys.* **35**, 795 (1963).

² E. Sheldon, *Phys. Letters* **2**, 178 (1962).

³ R. M. Humes and H. J. Hausman, *Phys. Rev.* **139**, B846 (1965).

Using inversion and rotation invariance, Yang⁴ has shown that for an unpolarized beam of incident particles, the angular correlation between the decay γ rays and the inelastically scattered particle group populating the decaying state has two symmetries: (1) The correlation is symmetric about the outgoing particle direction, in particular the correlation is independent of the propagation direction of the γ ray when that direction is confined to the surface of a cone whose axis coincides with the outgoing particle direction, and (2) in any plane containing the outgoing particle direction the angular correlation is symmetric about an axis perpendicular to the outgoing particle direction; that is, the γ distribution can be described by a polynomial containing only even powers of the cosine of the angle between the two radiations.

For the coordinate system shown in Fig. 1, the two model-independent symmetries of Yang may be expressed as follows:

(1) "Cone" symmetry:

$$W(\theta_p, \theta_\gamma, \phi_\gamma) = W(\theta_p, \theta_\gamma', \phi_\gamma'),$$

where θ_γ' is arbitrary except for the two restrictions

$$0 \leq \theta_\gamma' \leq \pi, \\ \theta_p - \theta_r \leq \theta_\gamma' \leq \theta_p + \theta_r,$$

where $\theta_r = \arccos[\cos\theta_p \cos\theta_\gamma + \sin\theta_p \sin\theta_\gamma \cos\phi_\gamma]$ is the angle between the particle and γ radiations and

$$\phi_\gamma' = \arccos \left[\frac{(\cot\theta_p)(\cos\theta_\gamma - \cos\theta_\gamma') + \sin\theta_\gamma \cos\phi_\gamma}{\sin\theta_\gamma'} \right].$$

In general, there will be two values of ϕ_γ' (two positions on the cone) for a given value of θ_γ' .

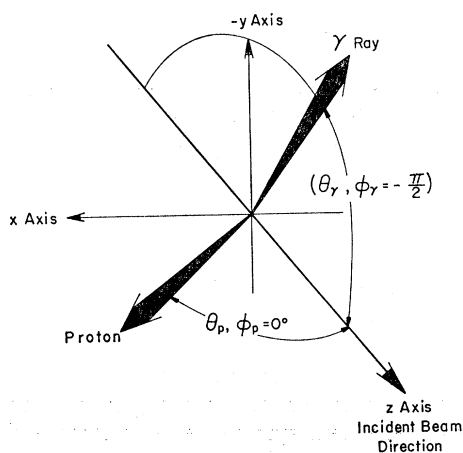


FIG. 1. The coordinate system used in describing the double-differential cross section for this experiment. The perpendicular correlations described in this paper refer to that geometry wherein γ -ray counter moves in the yz plane.

(2) "Plane" symmetry:

$$W(\theta_p, \theta_\gamma, \phi_\gamma) = W(\theta_p, \theta_\gamma', \pi - \phi_\gamma),$$

where

$$\theta_\gamma' = \arccos[(\cos\theta_\gamma - 2 \cos\theta_p \cos\theta_r) / (1 - \sin^2\theta_p \sin^2\phi_\gamma)].$$

Applying the plane and cone symmetries in sequence one finds what might be termed the "opposite γ " symmetry,

$$W(\theta_p, \theta_\gamma, \phi_\gamma) = W(\theta_p, \pi - \theta_\gamma, \phi_\gamma + \pi). \quad (1)$$

Thus, although the correlation function is dependent on the orientation of the line of motion of the γ ray it is independent of the direction of motion along that line.

The cone symmetry tells us that the correlation function is independent of the sign of ϕ_γ ,

$$W(\theta_p, \theta_\gamma, \phi_\gamma) = W(\theta_p, \theta_\gamma, -\phi_\gamma).$$

In particular, for γ rays detected in the y - z plane of Fig. 1 (a correlation so measured is hereafter referred to as a perpendicular correlation) this relation becomes

$$W(\theta_p, \theta_\gamma, \frac{1}{2}\pi) = W(\theta_p, \theta_\gamma, -\frac{1}{2}\pi).$$

Applying the opposite γ symmetry to the term on the left side of this equation we obtain the following model-independent perpendicular correlation symmetry:

$$W(\theta_p, \theta_\gamma, \pm \frac{1}{2}\pi) = W(\theta_p, \pi - \theta_\gamma, \pm \frac{1}{2}\pi). \quad (2)$$

The statistical CN symmetry for the perpendicular correlation has been shown by Sheldon to be

$$W(\theta_p, \theta_\gamma, \pm \frac{1}{2}\pi) = W(\pi - \theta_p, \theta_\gamma, \pm \frac{1}{2}\pi). \quad (3)$$

By measuring the particle- γ -ray correlations for two supplementary proton-detector angles, we have investigated the symmetry given in Eq. (3). Since all perpendicular correlations must be symmetric about the direction $\mathbf{k}_p \times \mathbf{k}_\gamma'$, any deviation from the CN symmetry given by Eq. (3) must be in the form of a change in magnitude of the correlation and not a change in shape. Deviations from the correlations predicted in Eq. (3) are to be investigated as resulting from direct-reaction channels.

In the past, much of the experimental angular correlation data reported was in the form of relative cross sections. Hence, reaction-model studies were concerned primarily with comparisons between model predictions and arbitrarily normalized experimental correlation shapes and symmetries. For a particular reaction proceeding primarily via compound-nucleus channels, even a small admixture of competing coherent direct channel could seriously distort the shape of the experimental correlation function without appreciably changing the absolute yield. By the same arguments, even for a reaction proceeding solely via the compound-nucleus channels, the statistical model correlation symmetries could be easily broken if only a small number of competing compound-nucleus states were involved in the reaction.

⁴ C. N. Yang, Phys. Rev. 74, 764 (1948).

In order to make a more critical confrontation between experiment and the predictions of reaction-model theories, we have measured our angular correlations as absolute double-differential cross sections, $d^2\sigma/d\Omega_p d\Omega_\gamma$. This permits us to study the details of the magnitudes of the predicted cross sections as well as the general symmetries. As another test of the statistical compound-nucleus model, we have also measured the spin-flip correlation, $W(\theta_p, \frac{1}{2}\pi, -\frac{1}{2}\pi)$, at three bombarding energies of 5.16, 5.25, and 5.46 MeV and compared the results with statistical theory.

II. THEORY

The directional correlation function for inelastic nucleon scattering by means of a statistical CN reaction mechanism has been developed by Satchler⁵ and generalized to include a spin-orbit interaction by Sheldon.² Let the inelastic scattering angular momentum sequence be denoted by $J_0(j_1)J_1(j_2)J_2(L, L')J_0$. This notation means that the target nucleus of spin J_0 captures a nucleon of total angular momentum j_1 to form a compound nucleus of spin J_1 , which in turn disintegrates into a nucleon of total angular momentum j_2 and an excited nucleus of spin J_2 . Finally, the latter returns to its ground state (spin J_0) by emitting γ radiation, which may be of mixed multipolarity L and L' with a mixing ratio Δ (the ratio of the reduced matrix elements for the L' and L transitions).

$$W(\theta_p, \theta_\gamma, \phi_\gamma) \sim \frac{d^2\sigma}{d\Omega_p d\Omega_\gamma} = \frac{\lambda^2}{32\pi} \frac{2J_2+1}{2J_0+1} \sum_{\mu\nu\lambda j_1 j_2 J_1} (-)^{2J_0-J_1-J_2+j_2} (2J_1+1)^2 (2j_1+1) (2j_2+1) \\ \times (j_1 j_1 \frac{1}{2} - \frac{1}{2} | \mu 0) (j_2 j_2 \frac{1}{2} - \frac{1}{2} | \nu 0) W(J_1 J_1 j_1 j_1; \mu J_0) [(2L+1)(LL-1 | \lambda 0) W(J_2 J_2 LL; \lambda J_0) \\ + 2\Delta(2L+1)^{1/2}(2L'+1)^{1/2}(LL'-1 | \lambda 0) W(J_2 J_2 LL'; \lambda J_0) + \Delta^2(2L'+1)(L'L'-1 | \lambda 0) \\ \times W(J_2 J_2 L'L'; \lambda J_0)] (1+\Delta^2)^{-1} X(J_1 J_1 \mu; j_2 j_2 \nu; J_2 J_2 \lambda) \tau(J_1 j_1 j_2) S_{\mu\nu\lambda}(\theta_p, \theta_\gamma, \phi_\gamma), \quad (5)$$

where μ , ν , and λ are even integers and the Legendre hyperpolynomial S has the form

$$S_{\mu\nu\lambda}(\theta_p, \theta_\gamma, \phi_\gamma) = 4\pi(2\mu+1)^{1/2}(2\lambda+1)^{-1/2} \\ \times \sum_m (-)^m (\mu \nu 0 m | \lambda m) Y_\nu^{-m}(\theta_p, 0) Y_\lambda^m(\theta_\gamma, \phi_\gamma),$$

where the Y_λ^m are the usual (Condon-Shortley) spherical harmonics.

Using the ALGOL language Sheldon and Gantenbein⁶ have written a computer program entitled BARBARA⁷ which evaluates the right-hand side of Eq. (5).

The proton angular distribution may be obtained by evaluating Eq. (5) with λ constrained to be zero,

$$\frac{d\sigma}{d\Omega_p} = \int \frac{d^2\sigma}{d\Omega_p d\Omega_\gamma} d\Omega_\gamma = 4\pi \left[\frac{d^2\sigma}{d\Omega_p d\Omega_\gamma} \right]_{\lambda=0}.$$

⁵ G. R. Satchler, Phys. Rev. **94**, 1304 (1954); **104**, 1198 (1956).
⁶ E. Sheldon and P. Gantenbein, J. Appl. Math. Phys. **18**, 397 (1967).

⁷ One of the authors (R. G. Seyler) has converted the language of this program to FORTRAN II.

There are two crucial assumptions of the statistical (or continuum) CN model. First, it is assumed that enough CN states of random phase are involved to yield zero average value for interferences of three types: (i) between different CN states, (ii) between different entrance partial waves, and (iii) between different exit partial waves. In terms of scattering amplitudes this means that

$$\langle S_{j_2 l_2 j_1 l_1}^{J_1 \pi_1} S_{j_2' l_2' j_1' l_1'}^{J_1' \pi_1'^*} \rangle_{Av} = |\bar{S}_{j_2 l_2 j_1 l_1}^{J_1 \pi_1}|^2 \\ \times \delta_{J_1 J_1'} \delta_{\pi_1 \pi_1'} \delta_{l_1 l_1'} \delta_{j_1 j_1'} \delta_{l_2 l_2'} \delta_{j_2 j_2'},$$

where l_i are orbital angular momenta, π_i is the parity of the CN state of spin J_1 and \bar{S} is an average scattering amplitude. Second, it is assumed that these average amplitudes depend only on the transmission coefficients $T_{ij}(E)$ of the partial waves (of energy E), and may be calculated by the equation

$$|\bar{S}_{j_2 l_2 j_1 l_1}^{J_1 \pi_1}|^2 = T_{l_1 j_1}(E_1) T_{l_2 j_2}(E_2) / \sum_{i l E} T_{ij}(E) \\ \equiv \tau(J_1 j_1 j_2), \quad (4)$$

where the sum is to be performed over all channels open to the particular CN state. The symbol $\tau(J_1 j_1 j_2)$ is introduced to abbreviate the above expression [Eq. (4)].

The directional correlation function derived under these assumptions is given by Sheldon as

As part of the input for the code BARBARA one must supply the penetrability or transmission coefficients, $T_{ij}(E)$, of the various partial waves at the energy E . These transmission coefficients may be obtained with the aid of the optical model. We used the optical-model search program of Auerbach called ABACUS-II.⁸ For the real non-spin-dependent part of the nuclear potential we employed the usual Saxon form factor, for the imaginary part the derivative of a Saxon form, and for the spin-orbit part, the familiar Thomas form.

Since some of the incident particle energies were above the (p, n) threshold it was necessary to obtain both neutron and proton transmission coefficients (see Fig. 2). The proton penetrabilities were calculated using the proton (local) optical-model parameters of Perey⁹: $V = 46.7 - 0.32E + ZA^{-1/3}$, $W' = 11$, $r_0 = r_0' = 1.25$,

⁸ Written by E. Auerbach and obtained from Brookhaven National Laboratory, Upton, Long Island, New York.

⁹ F. Perey, *Direct Interactions and Nuclear Reaction Mechanisms* (Gordon and Breach Science Publishers Inc., New York, 1963).

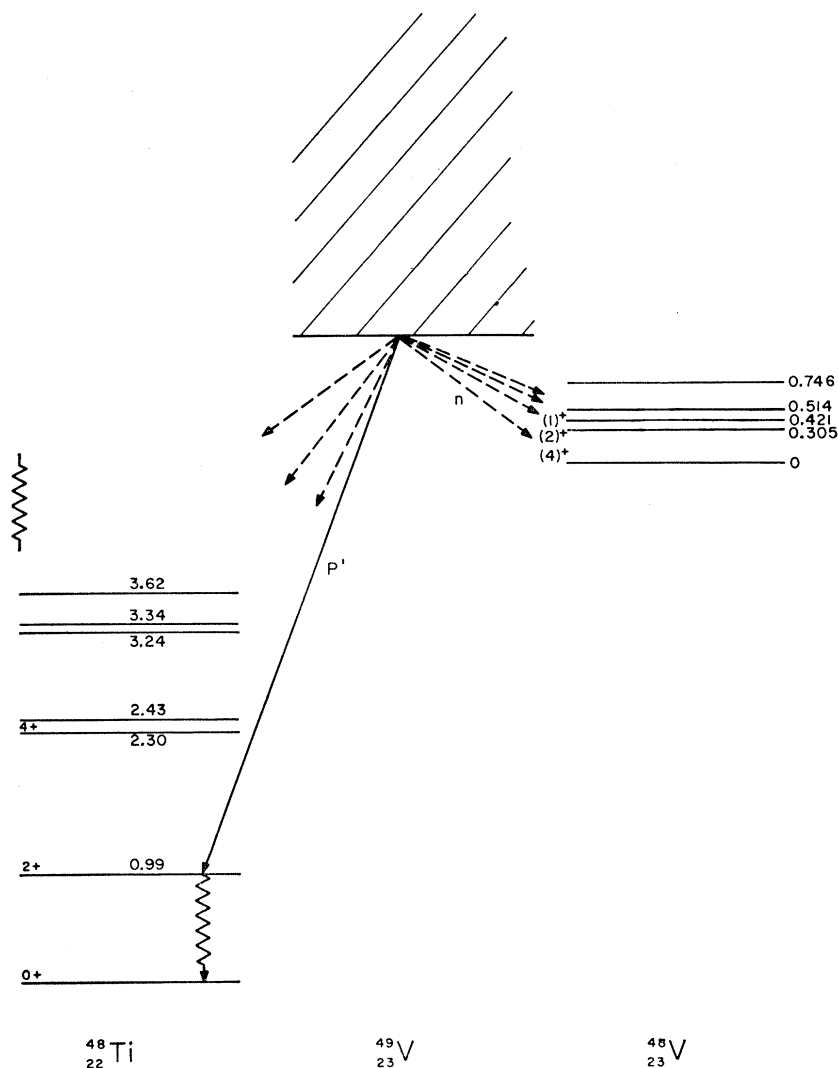


FIG. 2. Open-exit channels used in calculating the double-differential cross sections with the computer code BARBARA.

$a=0.65$, and $a'=0.47$, where the potential energies are in MeV (E is the center-of-mass energy) and the lengths are in fermi. These parameters were determined by Perey by studying the elastic scattering data in the 9–22-MeV range. It was assumed that the explicit energy dependence would permit the use of these parameters at even lower energies. For the neutron penetrabilities we used at each energy the local potential equivalent to the nonlocal neutron optical model of Perey and Buck.¹⁰ Equivalent here means that the two potentials yield the same elastic angular distribution. We used the local potential only because the code ABACUS-II has no provision for use of a nonlocal potential. The neutron (local) optical-model parameters used were: $V=48-0.29E$, $W'=10$ and r_0 , r_0' , a and a' are as given above for the proton potential. These neutron and proton parameters are the same as those used

by Sheldon.¹ The depth of the (real) spin-orbit potential (for both the neutron and proton) was taken as 7.5 MeV, which is close to the value used by Perey and Buck in their nonlocal neutron potential when one converts the latter value (1300 MeV) to pion units by multiplying it by $(m_\pi/2m_N)^2$.

The above-mentioned values of the optical potential parameters were *not* varied. That is, no attempt was made to find a set of optical parameters which would optimize the agreement between the code BARBARA predictions and the data. The quoted set of optical parameters was used as input for the code ABACUS-II, which produced the transmission coefficients. These coefficients and some additional information such as the angular momenta (in our case $J_0=0$, $J_2=L$, $\Delta=0$) and the incident energy were then used as input for the code BARBARA which produced as output the desired angular-correlation function.

¹⁰ F. Perey and B. Buck, Nucl. Phys. **32**, 353 (1962).

III. EXPERIMENTAL APPARATUS

The experimental arrangement is shown in Ref. 3. The beam from the Ohio State University 5.5-MeV Van de Graaff accelerator was magnetically analyzed and stabilized to 0.1% energy resolution. The beam was then bent through a switching magnet into the scattering chamber, where the beam was collimated to a spot of 0.040 in. diam. before striking the target. Finally, the beam was collected by the Faraday cup at the rear of the scattering chamber and integrated by a 0.1% current integrator.

The scattering chamber was a 0.063-in.-thick stainless-steel cylinder 10 in. in diam. with a hemispherical top to present uniform attenuating thickness to the γ rays. A solid-state detector, which was capable of being positioned remotely, was contained in the chamber for detection of the scattered charged particles. This detector was collimated to subtend 0.5×10^{-3} sr. Gamma rays were detected by a remotely positioned 3 in. \times 3 in. NaI(Tl) scintillator mounted on an RCA 8054 multiplier phototube located externally to the scattering chamber with the front face 17 cm from the target center. The positioning of this detector was accurate to $\pm 1.0^\circ$.

After being preamplified at the scattering chamber, the signals from both detectors were further amplified in the accelerator control room by Cosmic¹¹ double-delay line amplifiers which are part of our modular coincidence system. With a resolving time of 45 nsec a mean ratio of true-to-accidental counts of about 5:1 was obtained.

The target was a self-supporting foil obtained from the Oak Ridge National Laboratory ORNL as a separated isotope enriched to 99.36% Ti^{48} . The thickness was determined in two ways: by weighing a representative portion and by determining the shift in the $Li(p, n)$ threshold when the foil was inserted in the beam. The weighing method gave an average thickness of 0.929 ± 0.016 mg/cm² while the threshold shift indicated a thickness of 0.917 ± 0.037 mg/cm². The thickness was taken to be 0.923 ± 0.040 mg/cm² or approximately 40 keV at 4.6 MeV.

The double-differential cross sections $d^2\sigma/d\Omega_p d\Omega_\gamma$ have an over-all uncertainty of $\pm 8\%$ due primarily to uncertainties in the target uniformity ($\pm 5\%$) and in the efficiency solid-angle factor for the γ -ray detector ($\pm 5\%$). The error bars on the plotted experimental points are due solely to counting statistics and do not reflect the over-all absolute uncertainty. The plotted experimental points have been corrected for the finite geometry of the γ -ray detector using the calculations of Heath¹² and those of Herskind and Yoshizawa.¹³

Except for the 4.63- and 5.25-MeV correlation data, the perpendicular angular correlations were measured

with the proton detector at the two supplementary (in the center-of-mass coordinates) angles of 47° and 131° . For the 4.63-MeV perpendicular correlation, the supplementary proton-detector angles were 40° and 137° while for the 5.25-MeV data the supplementary proton-detector angles were 49° and 130° .

IV. RESULTS

Yield Curve

The relative yield of protons scattered inelastically from Ti^{48} leaving the residual nucleus in its first excited state at 0.99 MeV was measured at a laboratory proton-detector angle of 54° . The purpose of this measurement was to investigate the energy dependence of the yield curve over the bombarding energy available so as to determine those bombarding energies for correlation studies. As can be seen from the curve in Fig. 3, the yield curve shows many fluctuations over the energy region between $E_p = 3.7$ and 6.1 MeV. These fluctuations are broader on the average than the experimental energy spread of 40 keV. The positions of the peaks persists at other proton angles as can be seen in Fig. 4, and agree with the yield curves as measured by Seward¹⁴ and by Hulubei *et al.*¹⁵ The latter group have also made extensive angular correlation measurements for this reaction in the energy range of 4–8.5 MeV. The fact that the position of the peaks in the excitation curves persist over different detector angles seems to be evidence that these fluctuations are compound-nucleus resonances or clusters of overlapping resonances. We shall discuss this point further in Sec. V. After studying the yield curve, we elected to measure our angular correlations at 10 proton bombarding energies as indicated in Fig. 3 corresponding to peaks and valleys in the yield curve.

The absolute excitation function of the differential (p, p') cross section measured at one of the supplementary (c.m.) proton angles is shown in Fig. 4. The structure in the excitation curve is similar to that seen at a proton angle of 54° . The predictions of the statistical model, as computed using Sheldon's code BARBARA, are shown on the figure. The curve of most relevance is the one which was calculated taking into account all open proton and neutron channels for those levels shown in Fig. 2 which are energetically possible. The term "extra exit channels" is used in this and many subsequent figures. Our original CN calculations of the absolute double-differential cross sections were done using the program ERICA,¹⁶ which was compiled at ORNL by Sheldon. In this program it was assumed that only two exit channels were open, decays to the ground and first excited state. Subsequently, Sheldon¹⁷ revised his pro-

¹¹ Cosmic Radiation Labs., Inc., Bellport, New York.

¹² R. L. Heath, in *Scintillation Spectrometry Gamma-Ray Spectrum Catalogue* (Phillips Petroleum Company, 1964), 2nd ed.

¹³ B. Herskind and Y. Yoshizawa, Nucl. Instr. Methods **27**, 104 (1964).

¹⁴ F. D. Seward, Phys. Rev. **114**, 514 (1959).

¹⁵ H. Hulubei, A. Berinde, I. Neamu, N. Scintei, and N. Martalogu, Nucl. Phys. **89**, 165 (1966).

¹⁶ E. Sheldon, Oak Ridge National Laboratory Communication (unpublished).

¹⁷ E. Sheldon (private communication).

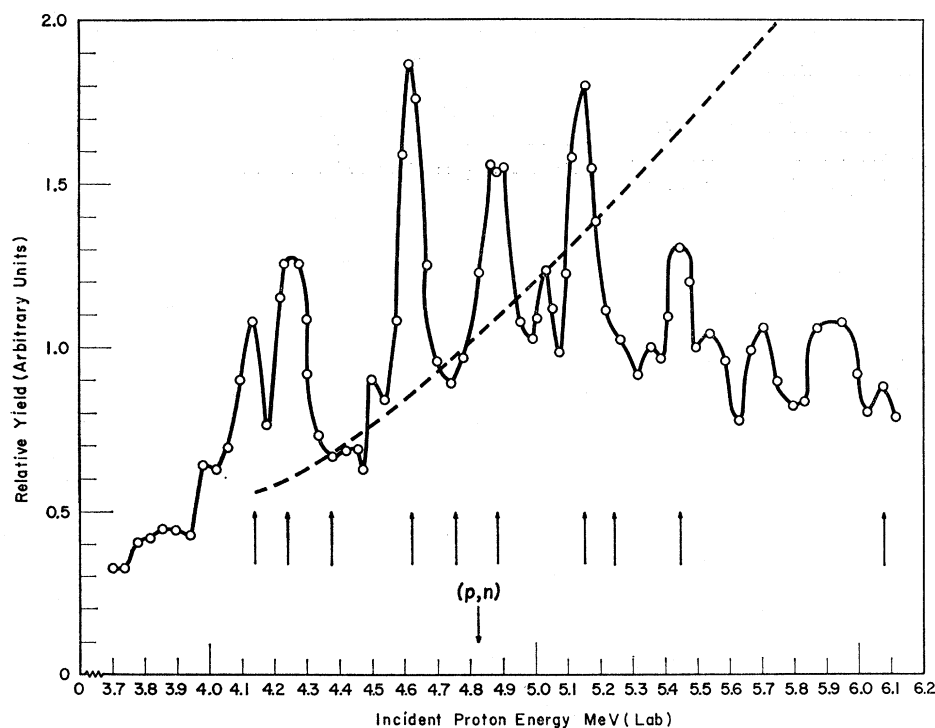


FIG. 3. Relative excitation curve for the protons leaving the residual nucleus Ti^{48} in its first excited state at 0.99 MeV. The proton-detector angle is 54° . The dashed curve is the calculated statistical CN yield assuming no extra exit channels. The arrows indicate energies at which the double-differential cross sections were measured. The solid line through the experimental points is added solely to guide the eye and is not a fit to the data.

gram to include the effects of all open exit channels energetically available to the reaction. The term "no extra channels" means that the open exit channels are assumed to be only the ground state and first excited state. Hence the term "5 extra channels" means that there are five open exit channels in addition to the ground state and first excited state. We have included both calculations in our figures in order to illustrate the

effect of the competing CN decay modes on the reaction under study. The energy levels for Ti^{48} and V^{49} used in these calculations were taken from the Landolt-Börnstein¹⁸ compilation tables. Although we subsequently found a more up-to-date determination of the Ti^{48} levels,¹⁹ we did not believe that the additional levels reported warranted the recalculation of the cross sec-

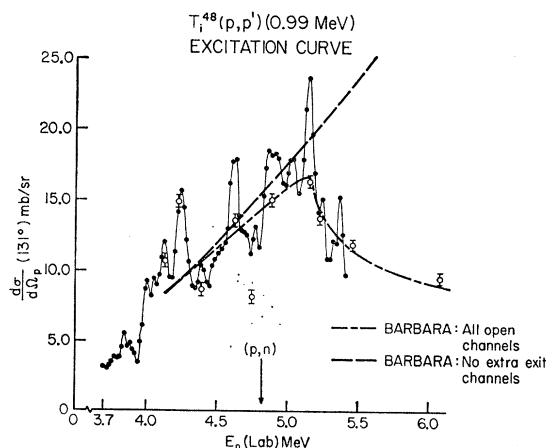


FIG. 4. The absolute excitation curve for protons leaving the residual nucleus Ti^{48} in its first excited state at 0.99 MeV. The proton-detector angle is 131° . The dashed curves are labelled on the figure and are the results of absolute statistical CN calculations using the code BARBARA. The solid line through the experimental points is added solely to guide the eye and is not a fit to the data. The experimental points with error flags are cross sections calculated from the measured angular correlations.

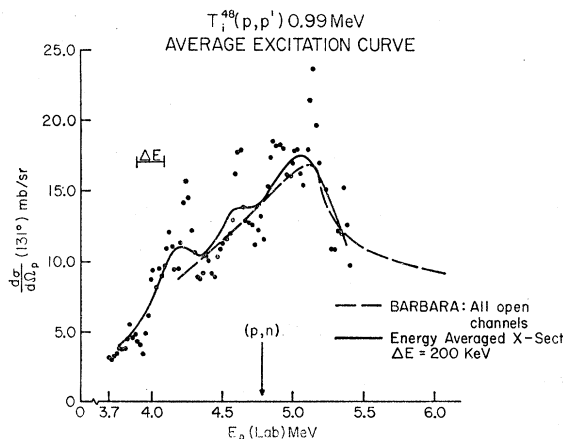


FIG. 5. The experimental points of the absolute excitation curve of Fig. 4 are plotted along with the solid curve representing the same excitation curve averaged over an energy interval of 200 keV. For comparison, the statistical CN predictions of the code BARBARA are also plotted as a dashed line.

¹⁸ Landolt-Börnstein, *Energy Levels of Nuclei A = 5 to A = 257* (Springer-Verlag, Berlin, 1961).

¹⁹ R. G. Arns (private communication); G. Brown, J. G. B. Haigh, and A. E. Macgregor, *Nucl. Phys.* **A97**, 353 (1967).

tions. In Fig. 5 we have plotted an average excitation curve using an energy interval of 200 keV and compared this curve with the predictions of the statistical model. Over this energy region the statistical model seems to account for practically all of the experimental yield.

The experimental points with error bars plotted in Fig. 4 are differential cross sections calculated from the absolute double-differential angular correlations measured at those energies. These cross sections are given by

$$\frac{d\sigma}{d\Omega_p} = \int_{\Omega_\gamma} \left(\frac{d^2\sigma}{d\Omega_p d\Omega_\gamma} \right) d\Omega_\gamma = 4\pi A_0, \quad (6)$$

where

$$\left(\frac{d^2\sigma}{d\Omega_p d\Omega_\gamma} \right)_{\text{exp.}} = \sum_{k=0,2,4} A_k P_k(\cos\theta),$$

and the A_k are determined by a least-squares fit to the experimental data. These calculations of the differential cross sections served as an internal check on the experimental conditions since we can compare the values of the excitation function obtained by two different

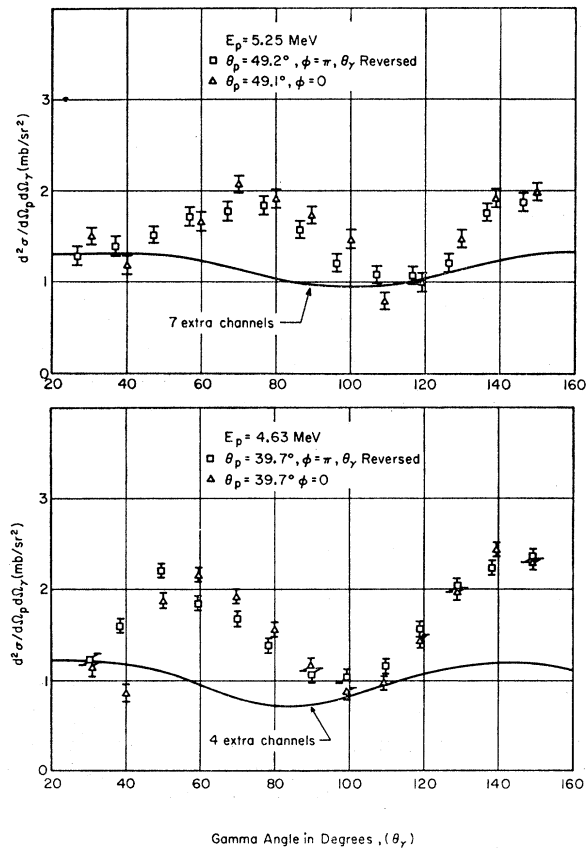


FIG. 6. Results of the absolute reaction-plane angular correlations which check the model-independent symmetry $W(\theta_p, \theta_\gamma, 0) = W(\theta_p, \pi - \theta_\gamma, \pi)$. The solid curve is the statistical CN computation using the code BARBARA.

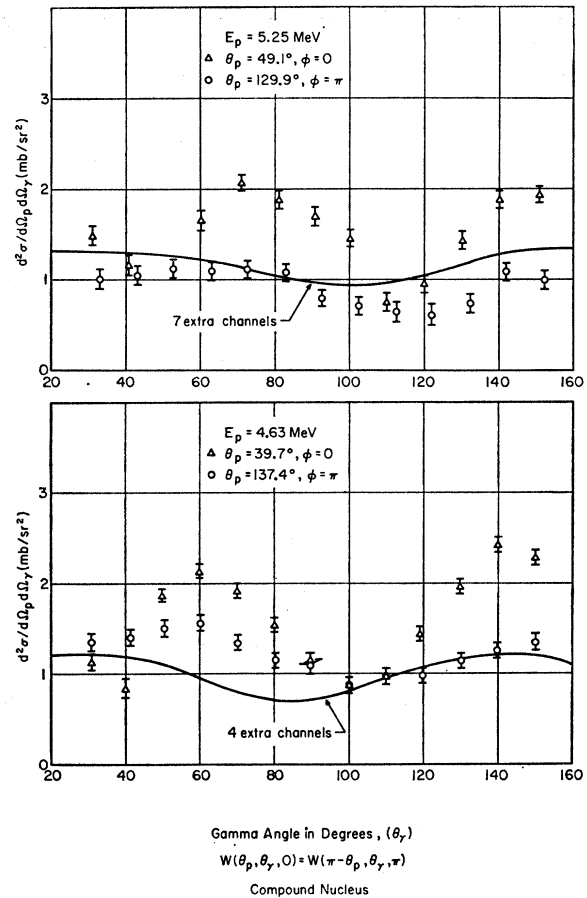


FIG. 7. Results of the absolute reaction-plane angular correlations which check the statistical CN symmetry $W(\theta_p, \theta_\gamma, 0) = W(\pi - \theta_p, \theta_\gamma, \pi)$. The solid curve is the statistical CN computation using the code BARBARA.

methods. Once the bombarding energy is above the (p, n) threshold, the statistical-model calculations give a reasonably accurate prediction of the reaction yield, allowing at most only a 15% direct-reaction yield.

Reaction-Plane Symmetries

The data in Figs. 6 and 7 is taken from the paper by Humes and Hausman³ and is reported here in order to compare the results with statistical-model calculations.

The first reaction-plane symmetry studied was the mechanism-independent symmetry of Eq. (1). For a fixed proton-detector angle, one angular correlation was measured with the γ -ray counter moving in the $\phi=0$ plane and another with the γ -ray detector moving in the $\phi=\pi$ plane. The results of the measurements, at two bombarding energies, plotted as absolute cross sections corrected for the finite geometry of the γ -ray detector, are shown in Fig. 6. In order to compare the predicted symmetry, the experimental points for the $\phi=\pi$ measurements were plotted such that the indicated θ_γ is $(\pi - \theta_\gamma)$. The indicated agreement with the predic-

tions of the model-independent symmetry serves more to establish a confidence level of the experimental equipment and procedures than as a test of an invariance rule. The predictions of the statistical-model code BARBARA, plotted as a solid curve in the figure, do not agree very well with the measured correlations.

The second reaction-plane symmetry studied at the two bombarding energies was the statistical CN symmetry,

$$W(\theta_p, \theta_\gamma, 0) = W(\pi - \theta_p, \theta_\gamma, \pi). \quad (7)$$

One of the angular correlations was measured with the proton detector at a fixed angle θ_p and with the γ -ray detector moving in the $\phi_\gamma = 0$ plane. The proton-detector angle was then changed to its supplementary (c.m.) angle $(\pi - \theta_p)$ and the γ -ray detector moved in the $\phi_\gamma = \pi$ plane.

Results of this measurement are shown in Fig. 7. Although the predicted compound-nucleus cross section agrees reasonably well with the cross section for the proton detector in the backward quadrant, it is obvious that the correlation does not agree with the symmetry predicted by Eq. (7). The breakdown of the predicted reaction-plane symmetry was one of the reasons we extended these measurements to the perpendicular ($\phi_\gamma = -\frac{1}{2}\pi$) plane.

Perpendicular-Plane Correlations

The results of the perpendicular-plane angular correlations ($\phi_\gamma = -\frac{1}{2}\pi$) are shown in Figs. 8 and 9. Measurements were made at a series of 10 laboratory bombarding energies as indicated by the arrows in Fig. 3. The data is displayed in two parts: the first (Fig. 8) is the absolute double-differential cross sections measured at bombarding energies corresponding to peaks in the yield curve; the second (Fig. 9) is the cross sections measured at bombarding energies corresponding to minima in the yield curve.

Within statistics, all of the perpendicular correlations were symmetric about the normal to the reaction plane in agreement with the predicted model-independent symmetry of Eq. (2). We used this predicted model-independent symmetry as a check on the experimental apparatus and alignment.

After the data were analyzed by least-squares fitting, it appeared (as seen in Figs. 8 and 9 and Table I) that the predicted compound-nucleus symmetry of Eq. (3) was broken more for those bombarding energies corresponding to peaks in the yield curve than for energies corresponding to minima in the yield curve. For this reason, we have presented our data in two figures. At each bombarding energy, angular correlations were measured for the proton detector at an angle θ_p and for the supplementary (c.m.) proton detector angle $(\pi - \theta_p)$. The absolute angular correlation coefficients for the data are summarized in Table I.

There are a number of interesting observations that can be made concerning these data. (1) Except for the

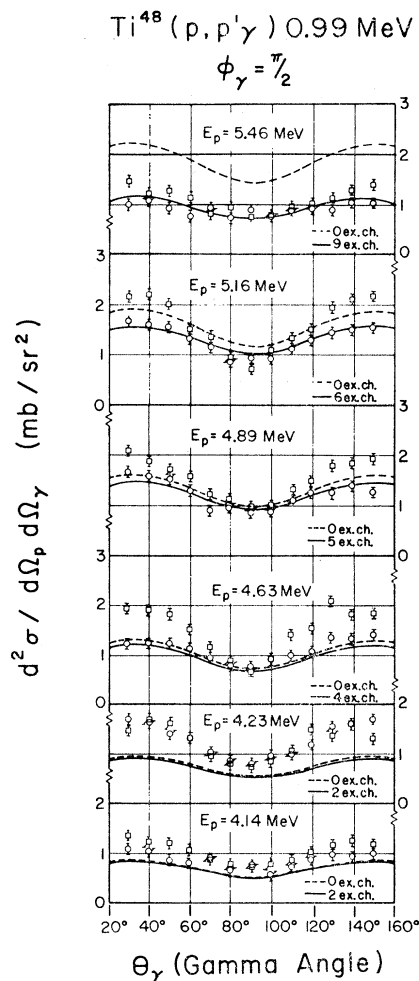


FIG. 8. The results of perpendicular-plane absolute angular correlations for six energies corresponding to peaks in the yield curve. The square data points correspond to angular correlations measured with the proton detector at an angle of 47° , while the circles correspond to data for the proton detector at the laboratory angle of 131° (supplementary in the center of mass). The solid curves are absolute double-differential cross sections calculated using the code BARBARA and accounting for all open exit channels. The dashed curves are BARBARA calculations assuming no extra exit channels.

bombarding energy of 4.76 MeV, the results of the statistical-model computations using BARBARA, and accounting for all open reaction channels, agree quite well with the measured correlations for that geometry wherein the proton-detector angle is in the backward quadrant. (2) At all bombarding energies the cross sections measured with the γ -ray detector along the direction perpendicular to the reaction plane (the so-called spin-flip direction) agree within statistics for the proton detector at both forward and backward angles, i.e.,

$$W(\theta_p, \frac{1}{2}\pi, -\frac{1}{2}\pi) = W(\pi - \theta_p, \frac{1}{2}\pi, -\frac{1}{2}\pi).$$

(3) At bombarding energies corresponding to peaks in the yield curve, the CN symmetry is broken and in all measurements the cross section is larger for the proton

detector in the forward quadrant rather than the backward quadrant.

It is the results of (3) that give us some hope that perpendicular correlations might be a sensitive test for measuring absolute direct-reaction contributions to this reaction. Direct reactions are generally characterized by a large forward scattering component. Consequently, the observation that the correlation yield is greater for the proton detector in the forward quadrant is consistent with the possibility of a direct-reaction contribution. It is tempting to speculate that the difference between the BARBARA prediction and the experimental yield might be due to such a direct contribution, but it is indeed perplexing that this difference is greater at bombarding energies corresponding to peaks in the yield curve rather than at the minima, for one might have argued that the peaks of the yield curve, where the CN contribution is the strongest would be the least likely place to observe direct-reaction contributions. On the other hand, the minima in the yield curve where CN resonances are smallest would be the most likely place to observe direct-reaction contributions. The results of our conclusions will be discussed more fully in Sec. V.

Spin-Flip Cross Section

Schmidt *et al.*²⁰ have recently pointed out some applications of a powerful theorem by Bohr²¹ concerning

TABLE I. Coefficients of the perpendicular correlations corrected for the finite size of the γ -ray detector:

$$d^2\sigma/d\Omega_p d\Omega_\gamma = \sum_{k=0,2,4} A_k P_k(\cos\theta) \quad (\text{mb/sr}^2).$$

E_p (MeV)	θ_p	A_0	A_2	A_4
4.14	47	1.00 ± 0.01	0.42 ± 0.04	-0.31 ± 0.06
	131	0.85 ± 0.02	0.32 ± 0.06	-0.13 ± 0.10
4.23	47	1.27 ± 0.02	0.71 ± 0.05	-0.31 ± 0.09
	131	1.19 ± 0.03	0.41 ± 0.09	-0.78 ± 0.13
4.38	47	0.73 ± 0.01	0.31 ± 0.03	-0.21 ± 0.06
	131	0.69 ± 0.02	0.20 ± 0.04	-0.17 ± 0.08
4.63	40	1.45 ± 0.02	0.80 ± 0.18	-0.79 ± 0.26
	137	1.08 ± 0.03	0.36 ± 0.11	-0.34 ± 0.14
4.76	47	0.77 ± 0.02	0.34 ± 0.04	-0.36 ± 0.07
	131	0.65 ± 0.02	0.15 ± 0.04	-0.39 ± 0.07
4.89	47	1.51 ± 0.02	0.78 ± 0.05	-0.37 ± 0.09
	131	1.19 ± 0.05	0.47 ± 0.19	-0.39 ± 0.28
5.16	47	1.58 ± 0.03	1.01 ± 0.09	-0.64 ± 0.13
	131	1.29 ± 0.02	0.62 ± 0.08	-0.26 ± 0.10
5.25	49.3	1.21 ± 0.05	0.59 ± 0.14	-0.63 ± 0.22
	130	1.10 ± 0.04	0.22 ± 0.12	-0.56 ± 0.19
5.46	47	1.11 ± 0.03	0.59 ± 0.11	0.03 ± 0.14
	131	0.91 ± 0.03	0.15 ± 0.12	-0.08 ± 0.16
6.08	47	0.91 ± 0.03	0.39 ± 0.08	-0.26 ± 0.12
	131	0.78 ± 0.02	0.36 ± 0.07	-0.08 ± 0.11

²⁰ F. H. Schmidt, R. E. Brown, J. B. Gerhart, and W. A. Kolanski, Nucl. Phys. **52**, 353 (1964).

²¹ A. Bohr, Nucl. Phys. **10**, 486 (1959).

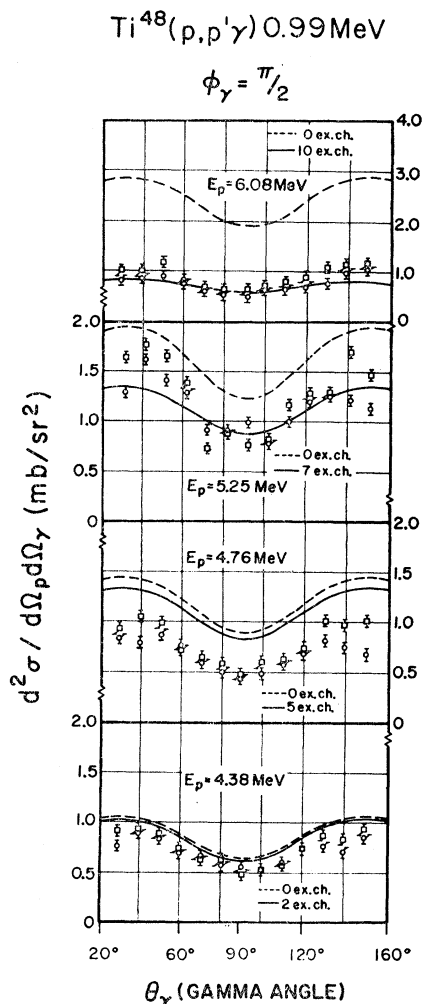


FIG. 9. The results of perpendicular-plane absolute angular correlations for four energies corresponding to valleys in the yield curve. As in Fig. 8, the square data points are for a proton-detector angle of 47° , the circle data points for the supplementary proton detector angle of 131° . The dashed curves are BARBARA calculations assuming no extra exit channels, while the solid curves are BARBARA calculations accounting for all open exit channels.

nuclear reactions. Bohr has shown that for a reaction invariant under the operation of reflection through the reaction plane, the following is true,

$$P_i \exp(i\pi S_i) = P_f \exp(i\pi S_f),$$

where P_i and P_f are the intrinsic parities of the initial and final systems and S_i and S_f are the sums of initial and final spin projections along the perpendicular to the reaction plane. Schmidt has shown that for a $0^+ \rightarrow 2^+ \rightarrow 0^+$ reaction only transitions from the $m = \pm 1$ magnetic substates (of the 2^+ state) can contribute to radiation along the normal to the reaction plane. For inelastic proton scattering, the population of the $m = \pm 1$ magnetic substates is uniquely associated with spin flip of the proton.

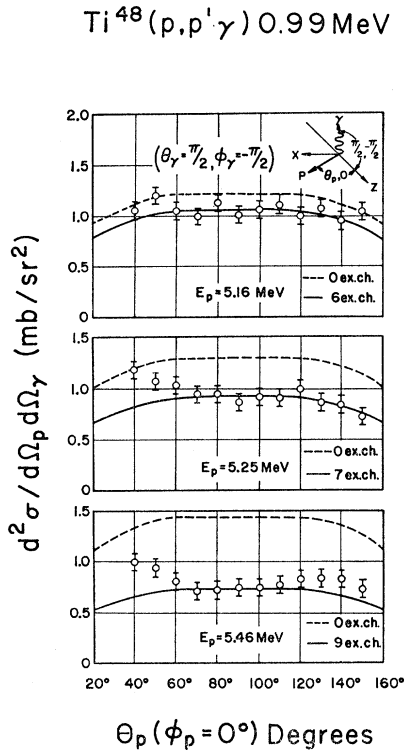


FIG. 10. Spin-flip angular correlations are shown as absolute double-differential cross sections at three proton bombarding energies. In the spin-flip geometry, the γ -ray detector is fixed along the direction perpendicular to the reaction plane. The curves are statistical CN calculations using the code BARBARA for zero- and all-open exit channels.

The results of the measured double-differential cross sections taken in the spin-flip geometry are shown in Fig. 10 for three proton bombarding energies. With the γ -ray detector fixed at a position normal to the reaction plane ($\theta_\gamma = \frac{1}{2}\pi$, $\phi_\gamma = -\frac{1}{2}\pi$), angular correlations were

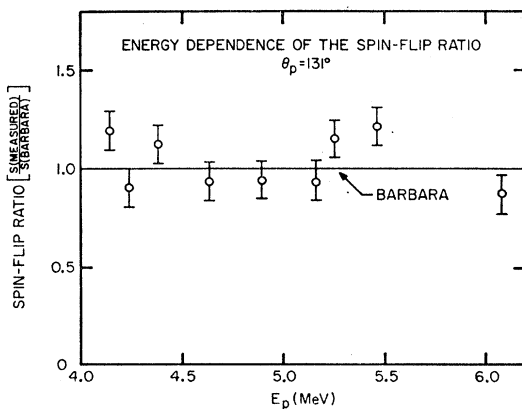


FIG. 11. The energy dependence of the spin-flip ratio is plotted for the case where the proton detector is at an angle of 131° . The measured spin-flip contribution was obtained from the data of Figs. 8 and 9. The spin-flip contribution is plotted as a ratio of the measured spin-flip cross section to the statistical CN spin-flip cross section.

measured for various proton-detector angles. The solid curves in the figure are the cross sections calculated using the code BARBARA.

The spin-flip probability has been shown by Schmidt to be

$$S = \frac{d^2\sigma(\theta_p, \frac{1}{2}\pi, -\frac{1}{2}\pi)}{d\Omega_p d\Omega_\gamma} \bigg/ \left(\frac{d\sigma}{d\Omega_p} \right) W_1(\theta_\gamma = \frac{1}{2}\pi, \phi_\gamma = -\frac{1}{2}\pi),$$

where W_1 is the distribution function for pure ($l=2$, $m=\pm 1$) radiation. In this relationship we have neglected the small (but finite) contribution of the radiations from the $m=\pm 2$ and $m=0$ substates which contribute radiation due to the finite size of the γ -ray detector.

In Fig. 11 we have chosen to plot the spin-flip probability as a ratio of measured-statistical-model calculations.

$$\text{Spin-flip ratio} = S(\text{measured})/S(\text{BARBARA}).$$

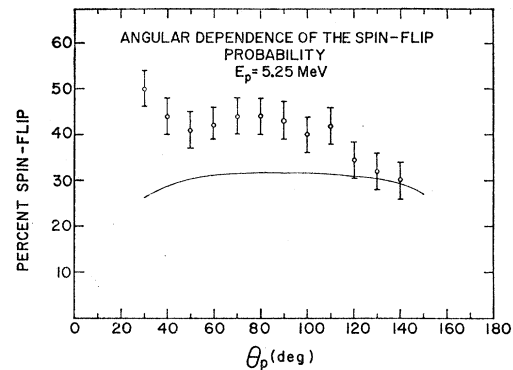


FIG. 12. The angular dependence of the spin-flip contribution to the reaction is plotted at a bombarding energy of 5.25 MeV. The solid curve is the spin-flip probability as calculated using the code BARBARA.

Figure 12 represents the angular dependence of the spin-flip probability at a bombarding energy of 5.25 MeV, the only energy at which both spin-flip cross sections and proton angular distributions were measured. Within statistics, the statistical compound-nucleus mechanism accounts for the spin-flip cross section for the backward quadrant. However, at the forward scattering angles, the measured spin-flip is almost twice the calculated compound-nucleus contribution. The latter result again suggests the presence of a direct-reaction contribution.

The energy dependence of the spin-flip ratio at a proton-detector angle of 131° is shown in Fig. 11. Over the energy range of interest, and within statistics, the statistical-compound-nucleus mechanism appears to satisfactorily account for the complete spin-flip part of the interaction. This result is not inconsistent with the observation of the angular dependence of the spin-flip ratio since the energy dependence was measured at a backward angle at $\theta_p = 131^\circ$.

V. DISCUSSION

How Statistical is "Statistical"?

One of the intests of this experiment was to investigate whether the relative contributions of CN and direct mechanisms could be deduced from the perpendicular correlations. In order to extract direct-reaction contributions from this reaction however, it is necessary to have reasonable assurances that the application of the statistical model is valid in this region of mass number and excitation energy (~ 11 MeV). Many previous experiments have shown that compound-nucleus reactions are dominant for bombarding energies near the classical Coulomb barrier energy such as in this experiment. However, unless one is dealing with a region of excitation energy wherein the excitation curve is composed either of individual isolated resonances or where one has a high density of overlapping resonant states, computations are very difficult. Consequently, titanium was chosen as a target nucleus with the expectation that at this mass number, level densities may be approaching those best described by the statistical model and yet the Coulomb barrier would not be greater than the bombarding energy available from our accelerator. Hence the first question to be answered is the following: "How valid is the assumption that the statistical model is a good approximation of the CN reaction at these excitation energies?"

A cursory glance at the yield curves of Figs. 3 and 4 gives little assurance of good statistical mixing. Over the energy range of interest there are a number of well-defined, intense, peaks which persist at both angles where excitation curves were measured. These peaks more nearly resemble the isolated resonances observed for light nuclei than the Ericson-type²² fluctuations observed in heavier nuclei and at higher excitation energies. However, level-density studies performed on nuclei in this mass range indicate level separations of ~ 5 keV, whereas the widths of the peaks in the Ti yield are approximately 100 keV. Consequently, it is likely that the peaks in the yield curve are not single isolated resonances. In Fig. 5 we have averaged the measured yield curve over an energy interval of 200 keV and compared this average yield curve to the predictions of BARBARA. It can be seen that for this energy interval, the statistical CN model gives excellent agreement with the averaged yield curve. This indicates that an experimental energy spread of 200 keV would have yielded more nearly those conditions approximating statistical averaging than the actual beam spread of 40 keV.

There have been a number of recent studies investigating the distribution of spacings of nuclear energy levels. One of these, most germane to the problem in question for this experiment, was recently reported by Huizenga and Katsanos.²³ They examined the experi-

mental spacing distribution for 980 nuclear levels of mixed spin and parity from 18 different nuclei in the mass range of $A = 36$ to 66. They report that the spacing distribution of the measured levels is essentially exponential in character in agreement with the prediction of randomly occurring levels of mixed spin and parity. The total number of levels up to excitation energy U is given by $N(U)$ which is fit with an equation of the form

$$N(U) = C e^{U/\tau},$$

where C and τ are constants derived for a particular excitation-energy range. We have obtained the constants $C = 2.7$, $\tau = 1.19$ MeV, by extrapolating the fits of Huizenga and Katsanos. Hence, for an excitation energy of 11.75 MeV (corresponding to a bombarding energy of 5 MeV), we obtain for the average level spacing in the CN V^{49} the value of 0.02 keV. These results predict approximately 1800 CN levels overlapped by our beam energy spread of 40 keV.

As a final test of the validity of the statistical model in describing this reaction, we can examine the success of the statistical model in predicting the double-differential cross sections measured in this experiment. With but a few exceptions, the statistical-model calculations using the code BARBARA are in excellent agreement both in magnitude and shape with the measured double-differential cross sections for those reactions wherein the proton detector is in the backward quadrant, $\theta_p = 131^\circ$. This is true for the measured yield curve, the perpendicular correlations, and the spin-flip cross section. It seems unlikely that such agreement would be accidental over such diverse experimental conditions.

In conclusion, it appears that even if there are not a statistically large number of levels within our beam energy spread, there are certainly a large number of levels. This gives us confidence that the statistical CN model gives a reasonable description of the measured correlations in this experiment. Assuming this to be true, we shall proceed to investigate how one might extract from the data that fraction of the reaction due to direct processes.

Direct-Reaction Contributions

For the measurements wherein the proton detector was in the forward quadrant at $\theta_p = 37^\circ$, the agreement between the BARBARA calculations and the measured perpendicular correlations is not very good, particularly at bombarding energies corresponding to peaks in the yield curve (see Fig. 8). There are a number of possible explanations that could account for these facts. We shall discuss two of these: (1) If within the experimental energy spread a statistically large number of (CN) overlapping levels of random phase were not excited, then interference effects between CN states might not average to zero, thus giving rise to asymmetries about 90° (c.m.) for the proton angular distributions and the angular correlations; (2) direct reactions are occurring

²² T. Ericson, Phys. Rev. Letters 5, 430 (1960).

²³ J. R. Huizenga and A. A. Katsanos, Nucl. Phys. A98, 614 (1967).

in this experiment and are contributing to the measured cross section. There is also the possibility of a combination of these two.

While it is of course impossible to rule out (1) completely, it is difficult to understand why this fact would not lead to disagreements between statistical CN prediction and experiment at all proton-detector angles. We have observed, however, that for the proton detector in the backward quadrant, the statistical CN predictions fit the measured correlations in both magnitude and shape. It is for those measurements wherein the proton detector is in the forward quadrant that agreement between calculations and measurements is poor. It is just this observation however that leads us to consider (2) as a real possibility since direct-reaction contributions tend to be peaked in the forward hemisphere and differences between the data and the statistical model predictions would, on the basis of (2), be expected to be larger at forward angles rather than at backward angles. Because of the statistical uncertainties in the data, the presence of a small direct contribution might not be experimentally detected at a backward proton-detector angle. However, because of the forward-peaking nature of direct reactions, even a small direct-reaction contribution might be experimentally detectable when the proton detector is in the forward quadrant.

An examination of Fig. 9 shows that at energies corresponding to valleys in the yield curve, the measured double-differential cross sections are essentially the same within statistics for the proton detector in both the forward and backward quadrant. It is only at bombarding energies corresponding to peaks in the yield curve wherein we observe the forward-backward asymmetry (see Fig. 8). Initially this was puzzling for we expected that the peaks of the yield curve where the CN contribution is the strongest would be the least likely place to observe the direct-reaction contributions, whereas the minima in the yield curve where CN contributions are weakest would be the most likely place to observe direct-reaction contributions. This supposition seems likely if the direct-reaction contributions are incoherent with the CN contributions so that the cross sections are additive. If, however, the direct and CN contributions are coherent, then one would expect to observe the maximum interference at those energies where the

amplitudes of either process are largest, i.e., the peaks of the yield curve. Of course such interference should occur whether the proton detector is in the forward or backward quadrant. However, if the direct contribution is small compared to the CN contribution, one might be unable to observe the interference experimentally with the proton detector in the backward quadrant.

The suggestion that the direct and CN contributions are coherent is however inconsistent with the statistical-model assumptions. The random-phase assumption of the statistical model implies that *all* interferences average to zero and thus there can be no interference between direct and CN contributions. Therefore, since interference is required to explain the symmetry breakdown for the correlation on the peaks, the basic assumptions of the statistical model cannot be completely satisfied for this reaction. We hope, in the near future, to be able to make quantitative determinations of the ratio of direct to CN contributions and the effects of the interference. As a gross upper limit to the direct-reaction contribution to this reaction, we can assume the contribution is incoherent with CN processes and subtract the double-differential cross sections for the forward and backward correlations. The results of this subtraction gives an average maximum direct-reaction contribution of about 15%.

Recently, Steiger²⁴ has measured reaction-plane angular correlations between neutrons inelastically scattered to the first excited state and de-excitation γ rays for the $Mg^{24}(n,n'\gamma)$ 1.37 MeV and $Fe^{56}(n,n'\gamma)$ 0.84 MeV reactions. His results also show a marked departure from the CN predicted symmetry for bombarding energies corresponding to maxima in the yield curves. In the case of the Fe^{56} reaction, Steiger indicates the likelihood of competition from the direct-reaction mechanism.

ACKNOWLEDGMENTS

We wish to thank Professor E. Sheldon for many fruitful ideas and particularly for his generosity in supplying us with the code BARBARA. We also wish to thank the staff of The Ohio State University Van de Graaff laboratory for their help throughout this work.

²⁴ M. P. Steiger, *Helv. Phys. Acta* **39**, 107 (1966).